

# Tunable Giant Rashba-type Spin Splitting in PtSe<sub>2</sub>/MoSe<sub>2</sub> Heterostructure

Longjun Xiang, Youqi Ke, and Qingyun Zhang\*

*School of Physical Science and Technology, ShanghaiTech University, Shanghai, 201210, China*

(Dated: May 4, 2022)

Finding materials with tunable and strong Rashba spin-orbit coupling is the central theme for realizing the Datta-Das spin field-effect transistor. In this work, we report a giant Rashba-type spin splitting in two-dimensional heterostructure PtSe<sub>2</sub>/MoSe<sub>2</sub> with first-principles calculations. We obtain large values of Rashba constant  $\alpha_R=1.3$  eV·Å and spin splitting energy  $E_R=150$  meV near Fermi level around  $\Gamma$  point, arising from the synergistic effect of structural inversion asymmetry and strong spin-orbit coupling. Moreover, we find the strong Rashba spin-orbit coupling in PtSe<sub>2</sub>/MoSe<sub>2</sub> can be significantly tuned by biaxial strain and external out-of-plane electrical field, presenting a promising material for the spin field-effect transistor. In addition, with the spin-valley physics at K/K' points in monolayer MoSe<sub>2</sub>, we propose a device model for spin field-effect transistor with opto-valleytronic spin injection based on PtSe<sub>2</sub>/MoSe<sub>2</sub> heterostructure.

The spin field-effect transistor (SFET) proposed by Datta and Das opens a door to information processing in future nanoelectronics.[1] The fundamental function of SFET is to modulate the current through the spin of electrons. In particular, the modulation is achieved by steering the spin precession with electrically tunable Rashba spin-orbit coupling (SOC)[2] in the channel materials of SFET.[3] The Rashba SOC is described by the Hamiltonian  $H_R=\alpha_R \boldsymbol{\sigma} \cdot (\mathbf{k}_{||} \times \mathbf{z})$ , in which  $\alpha_R$  is the Rashba constant representing the strength of SOC,  $\boldsymbol{\sigma}$  the vector of Pauli matrices,  $\mathbf{k}_{||}$  the in-plane wave vector of the electron, and  $\mathbf{z}$  the out-of-plane unit vector. Seeking suitable channel materials to fabricate SFET is the longstanding goal in the community of spintronics.[4, 5] A competent candidate should exhibit the following characteristics: (I) It holds a strong Rashba SOC reflected by large Rashba spin splitting energy  $E_R$ ; (II) Its Rashba constant  $\alpha_R$  can be effectively tuned with a gate voltage;[6, 7] (III) A Rashba electron system (*i.e.*, there are no other electronic states at Fermi level except for the Rashba states.) can be formed.[8]

In the past three decades, substantial theoretical and experimental efforts have been devoted to finding Rashba SOC at interfaces or surfaces. The Rashba-type spin splitting was observed in III-V semiconducting heterostructure InGaAs/InAlAs[6] with tiny Rashba constant ( $\alpha_R=0.001$  eV·Å). The surface states of heavy metals (*e.g.*, Au,[9] Bi,[10, 11] Ir,[12] Pb[13]) and topological insulator Bi<sub>2</sub>Se<sub>3</sub>[14, 15] exhibited large Rashba-type spin splittings. In addition, surface alloys, by doping heavy atoms at the surface of metals (*e.g.*, Bi/Ag(111)[16]) or semiconductors (*e.g.*, Bi/Si(111)[17] and Cs/InSb(110)[18]), provided an effective strategy to generate giant Rashba-type spin splitting. Typically, these observed Rashba-type surface states are accompanied with trivial surface states and spin degenerate bulk states, which hinders their practical applications. Recently, giant Rashba-type spin splittings

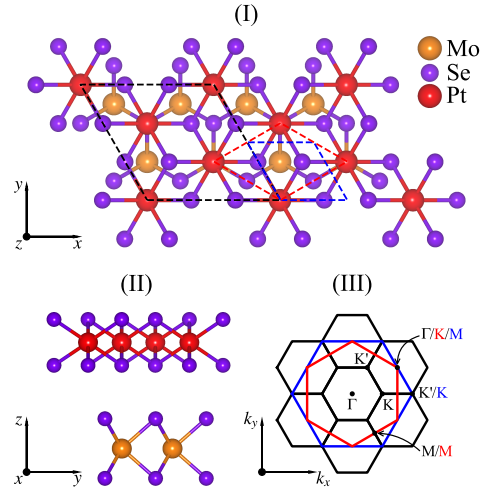


FIG. 1. (I) The top and (II) side view of the heterostructure PtSe<sub>2</sub>/MoSe<sub>2</sub>. (III) The corresponding Brillouin zones for the PtSe<sub>2</sub>/MoSe<sub>2</sub> heterostructure and their constituent monolayers.

were also observed in bulk BiTeI[19] and GeTe.[20, 21] However, it is unclear whether these effects can survive when the bulk materials are downscaled to a few atomic layers.[22] After the discovery of graphene,[23] two-dimensional (2D) materials and their van der Waals heterostructures[24–27] offer new opportunities to search for materials with Rashba SOC.[5] For example, the Rashba effect was predicted in the monolayer LaOBiS<sub>2</sub> ( $\alpha_R=3.04$  eV·Å,  $E_R=38$  meV)[28] and BiSb ( $\alpha_R=2.3$  eV·Å,  $E_R=13$  meV).[29] By stacking Bi<sub>2</sub>Se<sub>3</sub> ultrathin film on MoTe<sub>2</sub> substrate, Wang *et al.*[8] predicted a wide-range Rashba electron gas ( $\alpha_R=0.67$  eV·Å,  $E_R=8$  meV). The Rashba effect was also predicted in the van der Waals heterostructure BiSb/AlN ( $\alpha_R=1.1$  eV·Å,  $E_R=5$  meV)[29] and GaSe/MoSe<sub>2</sub> ( $\alpha_R=0.49$  eV·Å,  $E_R=31$  meV).[30] Despite these important progresses, challenges still exist in these predicted systems, such as the thermal stability, electric tunability, and the small Rashba energy

\* zhangqy2@shanghaitech.edu.cn

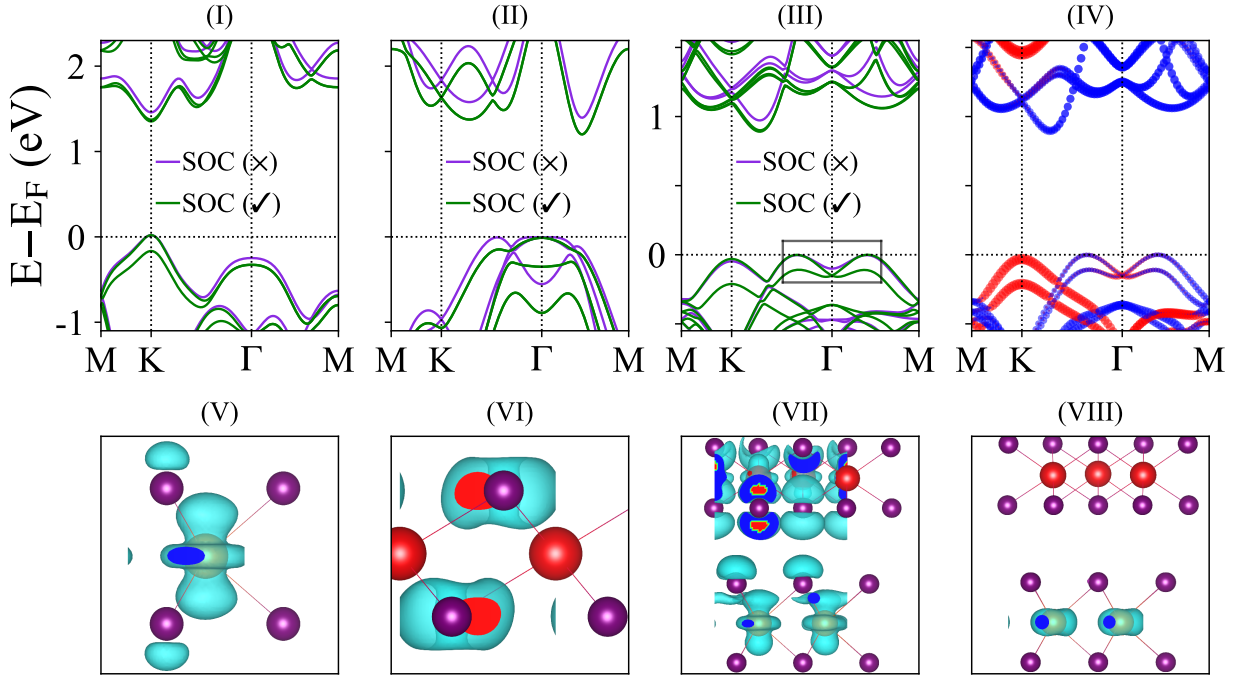


FIG. 2. Band structures of (I) monolayer MoSe<sub>2</sub>, (II) monolayer PtSe<sub>2</sub>, and (III) heterostructure PtSe<sub>2</sub>/MoSe<sub>2</sub> without (blueviolet) and with (green) spin-orbit coupling. (IV) Layer-projected band structure for PtSe<sub>2</sub>/MoSe<sub>2</sub>, in which the red and blue circles represent the respective contributions from MoSe<sub>2</sub> and PtSe<sub>2</sub>. The charge densities of VBE around  $\Gamma$  point for (V) monolayer MoSe<sub>2</sub>, (VI) monolayer PtSe<sub>2</sub>, (VII) heterostructure PtSe<sub>2</sub>/MoSe<sub>2</sub>, and (VIII) at K point for PtSe<sub>2</sub>/MoSe<sub>2</sub>. The isosurface values of 0.005 and 0.0005 electron/Å<sup>3</sup> are adopted for monolayers and heterostructure, respectively.

$E_R$ . Therefore, further efforts are required to search for more appropriate materials for SFET.

Very recently, the semiconducting T-phase transition metal dichalcogenide (TMDC) PtSe<sub>2</sub> monolayer has attracted much attention due to its superior transport properties.[31, 32] Moreover, Yao *et al.*[33] observed the spin-layer locking phenomena[34, 35] induced by local dipole field in this material, which manifests the significant role of SOC. However, the degeneracy protected by inversion symmetry in PtSe<sub>2</sub> impedes its applications to SFET. To lift the degeneracy the structural inversion asymmetry should be introduced, for example, by substitutional doping.[36] However, we note that building van der Waals heterostructure is more favorable in experiment compared to the doping method. On the other hand, monolayer H-phase TMDCs, such as MoSe<sub>2</sub>, have been exfoliated successfully and also possess strong SOC.[37, 38] Therefore, the heterostructure stacked by T-phase and H-phase TMDCs monolayer, with broken inversion symmetry, provide a promising platform for studying spin physics. In this work, we investigate the electronic properties of the van der Waals heterostructure PtSe<sub>2</sub>/MoSe<sub>2</sub> through first-principles calculations. We find that the spin-valley physics[39] at K/K' points from H-phase MoSe<sub>2</sub> are preserved. Interestingly, a giant Rashba-type spin splitting ( $\alpha_R=1.3$  eV·Å,  $E_R=150$  meV) near Fermi level around  $\Gamma$  point is observed. Furthermore, we demonstrate that a 2D Rashba electron system

can be obtained by tuning the biaxial strain and external out-of-plane electrical field. Moreover, the Rashba constant  $\alpha_R$  exhibits an almost linear dependence on the external electrical field, which implies that the spin can be effectively manipulated with a gate voltage. Finally, based on the spin-valley physics and the tunable giant Rashba-type spin splitting, we propose a SFET model with opto-valleytronic spin injection.[40]

All the calculations are performed with density functional theory (DFT) by the projector-augmented wave (PAW) method implemented in the Vienna Ab initio Simulation Package (VASP)[41]. The generalized gradient approximation as parametrized by Perdew, Burke, and Ernzerhof (PBE)[42] is employed. The kinetic energy cutoff 460 eV and a  $\Gamma$ -centered  $6 \times 6 \times 1$  k-mesh in 2D Brillouin zone have been used for the convergence of total energy with a criterion of  $1 \times 10^{-6}$  eV per atom. The SOC is not included during the geometry optimization but is added in the electronic structure calculations. The relaxed lattice constants of MoSe<sub>2</sub> and PtSe<sub>2</sub> are 3.286 Å and 3.780 Å, respectively. To minimize the artificial internal strain caused by lattice mismatch, the heterostructure is built from  $\sqrt{3} \times \sqrt{3} \times 1$  supercell of PtSe<sub>2</sub> and  $2 \times 2 \times 1$  supercell of MoSe<sub>2</sub>, as shown in Fig.1 (I), and both the lattice vectors and atomic positions of the heterostructure are fully relaxed to further reduce the artificial strain. A vacuum space of 20 Å is adopted to avoid the interaction between two periodic slabs along

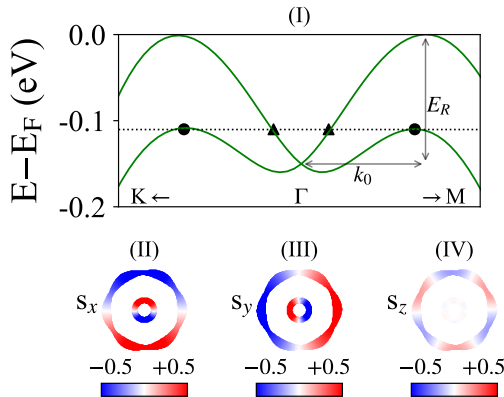


FIG. 3. (I) The two zoom-in Rashba splitting bands around  $\Gamma$  point, the Rashba energy  $E_R$  and Rashba momentum  $k_0$  are labeled explicitly. (II)-(IV) Three spin components in the 2D Brillouin zone centered on  $\Gamma$  point at a constant-energy cut labeled by the dashed line in (I), in which the crossings of inner, outer contours with the plotted  $k$ -path are marked by black triangles and dots, respectively.

[001] direction. The DFT-D3[43] method has been applied to simulate the van der Waals interaction and the relaxed interlayer distance is 3.228 Å.

In Fig.2 (I-III), we present the band structures for monolayer MoSe<sub>2</sub>, monolayer PtSe<sub>2</sub>, and their heterostructure without/with SOC. The Fermi level is set to valence band maximum (VBM) in all band structures. As shown in Fig.2 (I)-(II), the pristine monolayers MoSe<sub>2</sub>[44] and PtSe<sub>2</sub>[31] are direct and indirect semiconductors, respectively. When SOC is considered, the bands of monolayer MoSe<sub>2</sub> (PtSe<sub>2</sub>) are split (not split) along M-K- $\Gamma$   $k$ -path due to the absence (presence) of inversion symmetry. The heterostructure PtSe<sub>2</sub>/MoSe<sub>2</sub> is coupled by weak van der Waals interaction, therefore, the band structure of PtSe<sub>2</sub>/MoSe<sub>2</sub> should preserve most of the characteristics of its constituent monolayers. As expected, the heterostructure PtSe<sub>2</sub>/MoSe<sub>2</sub> retains the semiconducting nature with an indirect band gap 0.89 eV when SOC is considered, as shown in Fig.2 (III). In addition, the heterostructure also preserves the large spin splitting (181 meV) at K point with a slight reduction in comparison with the spin splitting in monolayer MoSe<sub>2</sub> (186 meV). Interestingly, an emerging band splitting around  $\Gamma$  point is observed, which does not appear in the constituent monolayers. To unveil the physical origins of the band splittings around  $\Gamma$  point, we firstly investigate the layer-projected band structure, as shown in Fig.2 (IV). The contribution from monolayer MoSe<sub>2</sub> and PtSe<sub>2</sub> are indicated by red and blue circles, respectively. From the projected band structure, we observe an important hybridization from two constituent monolayers at the valence band edge (VBE) around  $\Gamma$  point. Compared to previous studies of bilayer MoS<sub>2</sub> and heterostructure MoSe<sub>2</sub>/MoS<sub>2</sub>[45-47], in which the hybridization around  $\Gamma$  point is dominated by Mo-*d* orbitals

(see Fig.1 in the supplementary materials), the observed hybridization around  $\Gamma$  point in PtSe<sub>2</sub>/MoSe<sub>2</sub> displays a distinct feature: it is mainly contributed by Mo-*d* orbitals in MoSe<sub>2</sub> and Se-*p* orbitals in PtSe<sub>2</sub>. The hybridization causes the redistribution of charge at the interface between PtSe<sub>2</sub> and MoSe<sub>2</sub>, breaks the inversion symmetry and hence induces a vertical interfacial electrical field which leads to the band splitting around  $\Gamma$  point. In addition, we note that the MoSe<sub>2</sub> layer is responsible for the band splitting around K point at VBE with an only minor influence from PtSe<sub>2</sub> layer. Different from the behavior at VBE, the states at conduction band edge (CBE) are dominated by PtSe<sub>2</sub>, presenting a mixed type-I and type-II band alignment.[48] Furthermore, to capture more details of the band splitting around  $\Gamma$  point, the band decomposed charge densities are plotted, as shown in Fig.2 (V-VII). For monolayer PtSe<sub>2</sub> and MoSe<sub>2</sub>, the charge density around  $\Gamma$  point has an equal contribution from top and bottom Se layers, therefore, the total vertical electrical field acting on the electrons is canceled and no band splitting is observed. While for PtSe<sub>2</sub>/MoSe<sub>2</sub>, the charge density around  $\Gamma$  point displays the features of  $d_{z^2}$  orbital of Mo atom and  $p_z$  orbital of Se atom, as shown in Fig.2 (VII). Moreover, the charge densities from Se-*p* orbitals are mainly distributed in the interfacial region, experiencing an unbalanced vertical electric field generated by surrounding atoms, which is responsible for the band splitting around  $\Gamma$  point. As a comparison, in Fig.2 (VIII) we also plot the charge density of VBE at K point, which is dominated by  $d_{xy}$  orbital and  $d_{x^2-y^2}$  orbital of Mo atom, same as the monolayer MoSe<sub>2</sub>.[39]

It's thus clear that the band splitting around  $\Gamma$  point is an emerging property of the heterostructure, given by the important *p-d* orbital hybridization between MoSe<sub>2</sub> and PtSe<sub>2</sub>. By zooming in the two highest valence bands around  $\Gamma$  point in Fig.3 (I) (marked by the black rectangular box in Fig.2 (III)), we note that our results exhibit close resemblance to the Rashba-type spin splittings in semiconductor quantum wells and surfaces of heavy metals.[6, 9-12, 16, 17] To further confirm that the observed band splitting is Rashba-type, we calculate the spin components  $s_x$ ,  $s_y$  and  $s_z$  at the constant energy marked by the dashed line in Fig.3 (I). As illustrated in Fig.3 (II)-(IV), the spin polarizations are mainly in-plane:  $s_x$  and  $s_y$  are significantly larger than the  $s_z$ , and furthermore, the inner contours show a helical spin polarization opposite to the outer contours. Such spin texture is the iconic feature of the Rashba effect. The small out-of-plane spin component  $s_z$  in Fig.3 (IV) is owing to the small in-plane potential gradient, which is also responsible for the hexagonal shape of the outer contour.[9, 10] Although the split subbands are not exactly parabolic as predicted by original Rashba Hamiltonian, the relation  $\alpha_R=2E_R/k_0$  still gives a reasonable estimation for the Rashba constant. From Fig.3 (I) we obtain the Rashba energy  $E_R=150$  meV and Rashba momentum  $k_0=0.23$  Å<sup>-1</sup>, giving the Rashba constant  $\alpha_R=1.3$  eV·Å. The obtained value is one of the largest among the Rashba

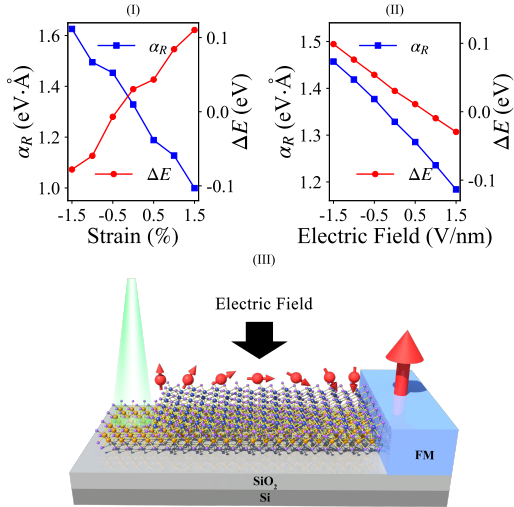


FIG. 4. (I-II) The Rashba constant  $\alpha_R$  and the relative energy shift  $\Delta E$  (between K and the highest point around  $\Gamma$ ) versus the biaxial strains from  $-1.5\%$  (compression) to  $1.5\%$  (expansion) and external electric fields from  $-1.5$  eV/nm to  $1.5$  eV/nm. (III) The schematic illustration of spin injection with circularly polarized photons, lateral spin transport with electrically tunable Rashba-type effect and spin detection with ferromagnetic contact.

splittings observed in previous studies.[6, 9–12, 16, 17]

To check whether the Rashba effect appears in other PtX<sub>2</sub>/MX<sub>2</sub> (M=Mo, W; X=S, Se, Te) heterostructures except for PtSe<sub>2</sub>/MoSe<sub>2</sub>, we also perform the calculations for the five other heterostructures (see Fig.2 and Fig.3 in the supplementary materials). The band structure and orbital characteristics of PtS<sub>2</sub>/MoS<sub>2</sub> are similar with those of PtSe<sub>2</sub>/MoSe<sub>2</sub>, while the band gap is larger and the Rashba spin splitting is much smaller, which is attributed to the weaker SOC in S atoms. However, there is almost no orbital hybridization between MoTe<sub>2</sub> and PtTe<sub>2</sub> at VBE around  $\Gamma$  point, hence no band splitting is observed. Substituting Mo atoms with W atoms in these heterostructures will bring about two main changes to their band structures. Firstly, the band splittings of VBE at K point become larger due to the stronger SOC in W atom than that in Mo atom. Secondly, the energy levels of VBE around  $\Gamma$  point is suppressed compared to those at K point. Therefore, from the application point of view, the PtSe<sub>2</sub>/MoSe<sub>2</sub> heterostructure is the most promising candidate in the PtX<sub>2</sub>/MX<sub>2</sub> family for SFET.

As outlined at the beginning of the paper, strong Rashba SOC is only one of the prerequisites to realize SFET. Next, we investigate the tunability of electronic properties of PtSe<sub>2</sub>/MoSe<sub>2</sub> heterostructure under biaxial strain and external electric field. At first, we impose biaxial strains from  $\delta=-1.5\%$  (compression) to  $\delta=1.5\%$  (tension) on the heterostructure, in which the strength of the strain is described by  $\delta=(a-a_0)/a_0$  with  $a_0$  the original lattice constant. For different strains, the electronic structures are calculated after all the atoms are fully re-

laxed. In particular, we investigate the Rashba constant  $\alpha_R$  and the relative energy shift  $\Delta E = E_\Gamma - E_K$  between the VBM around  $\Gamma$  point and at K point, as shown in Fig.4 (I). It is found that the Rashba constant  $\alpha_R$  (in blue squares) is decreased from  $1.62$  eV·Å to  $1.00$  eV·Å as  $\delta$  is changed from  $-1.5\%$  to  $+1.5\%$ . In the meanwhile, the relative energy shift  $\Delta E$  is increased. The notably increasing  $\Delta E$  means that the position of VBM near  $\Gamma$  point will be elevated gradually relative to that at K point with the tensile strains. The results manifest that the tensile strain provides an effective approach to generate a Rashba electron system. When applying an external electric field from  $-1.5$  (V/nm) to  $1.5$  (V/nm) along  $z$  direction, the  $\alpha_R$  and  $\Delta E$  are reduced at the same time, as shown in Fig.4 (II), which means the external electric field also can promote the VBM near  $\Gamma$  point above K point to create a Rashba electron system. Furthermore, the Rashba constant exhibits a notable change (24%) from  $1.46$  eV·Å to  $1.18$  eV·Å when the external electric field is changed from  $-1.5$  (V/nm) to  $1.5$  (V/nm), indicating that the spin precession can be effectively tuned with a gate voltage. Since the phase difference of spin precession angle is given by[7]  $\Delta\theta = 2m^*\Delta\alpha_R L/\hbar^2$  ( $\Delta\alpha_R$  represents the changes of the Rashba constant,  $m^*$  is the effective mass and  $L$  the distance between spin injector and detector), the appreciable tunability of the Rashba constant  $\alpha_R$  is crucial for realizing spin transport in ballistic regime. Finally, based on the tunable giant Rashba-type spin splitting in PtSe<sub>2</sub>/MoSe<sub>2</sub> heterostructure and the valley physics from H-phase monolayer MoSe<sub>2</sub>, we propose a theoretical model of SFET, illustrated in Fig.4 (III). Similar to the SFET designed by Luo *et al.*,[40] the valley polarization at K/K' points in MoSe<sub>2</sub> is utilized to achieve spin injection. However, in our mode the spin transport with designed precession is completed with a gate voltage rather than the magnetic field along the transport direction. It is worth noting that since the spin precession angle is independent of energy[1], heavy hole doping in PtSe<sub>2</sub>/MoSe<sub>2</sub> heterostructure is not necessary for SFET application.

In summary, we investigate the electronic properties of the PtSe<sub>2</sub>/MoSe<sub>2</sub> heterostructure through density functional theory calculations. A giant Rashba-type spin splitting ( $\alpha_R=1.3$  eV·Å,  $E_R=150$  meV) near Fermi level is predicted, arising from structural asymmetry and strong spin-orbit coupling. Furthermore, we explore the tunability of electronic structure under biaxial strain and external electrical field. The results manifest that both biaxial strain and external electric field can be utilized to achieve a 2D Rashba electron system. Furthermore, the Rashba constant  $\alpha_R$  can be tuned effectively by the external electrical field, which enables the control of spin degree of freedom with a gate voltage. Combining the tunable giant Rashba-type spin splitting around  $\Gamma$  in PtSe<sub>2</sub>/MoSe<sub>2</sub> and the valley-physics from H-phase monolayer MoSe<sub>2</sub>, we propose a theoretical model of SFET. Since monolayer PtSe<sub>2</sub> and MoSe<sub>2</sub> have already been fabricated in experiment and proven to be air-stable at

room temperature, it should not be difficult to prepare PtSe<sub>2</sub>/MoSe<sub>2</sub> heterostructure and realize the proposed SFET.

## ACKNOWLEDGEMENTS

Y.K. thanks the financial support from the ShanghaiTech University start-up fund, The Thousand Young Talents Plan and Shanghai Shuguang Plan. Q.Z. thanks the support from NSFC with grant No. 11704121.

---

[1] S. Datta and B. Das, Electronic analog of the electrooptic modulator, *Applied Physics Letters* **56**, 665 (1990).

[2] Y. A. Bychkov and É. I. Rashba, Properties of a 2D electron gas with lifted spectral degeneracy, *JETP lett* **39**, 78 (1984).

[3] S. Datta, How we proposed the spin transistor, *Nature Electronics* **1**, 604 (2018).

[4] I. Zutic, J. Fabian, and S. Sarma, Spintronics: Fundamentals and applications, *Rev. Mod. Phys.* **76**, 323 (2004).

[5] A. Manchon, H. C. Koo, J. Nitta, S. Frolov, and R. Duine, New perspectives for Rashba spin-orbit coupling, *Nature materials* **14**, 871 (2015).

[6] J. Nitta, T. Akazaki, H. Takayanagi, and T. Enoki, Gate control of spin-orbit interaction in an inverted In<sub>0.53</sub>Ga<sub>0.47</sub>As/In<sub>0.52</sub>Al<sub>0.48</sub>As heterostructure, *Phys. Rev. Lett.* **78**, 1335 (1997).

[7] P. Chuang, S.-C. Ho, L. W. Smith, F. Sfigakis, M. Pepper, C.-H. Chen, J.-C. Fan, J. P. Griffiths, I. Farrer, H. E. Beere, G. A. C. Jones, D. A. Ritchie, and T.-M. Chen, All-electric all-semiconductor spin field-effect transistors, *Nature Nanotechnology* **10**, 35 (2015).

[8] T.-H. Wang and H.-T. Jeng, Wide-range ideal 2D Rashba electron gas with large spin splitting in Bi<sub>2</sub>Se<sub>3</sub>/MoTe<sub>2</sub> heterostructure, *npj Comput. Mater.* **3**, 5 (2017).

[9] S. LaShell, B. A. McDougall, and E. Jensen, Spin splitting of an Au(111) surface state band observed with angle resolved photoelectron spectroscopy, *Phys. Rev. Lett.* **77**, 3419 (1996).

[10] Y. M. Koroteev, G. Bihlmayer, J. E. Gayone, E. V. Chulkov, S. Blügel, P. M. Echenique, and P. Hofmann, Strong spin-orbit splitting on Bi surfaces, *Phys. Rev. Lett.* **93**, 046403 (2004).

[11] T. Hirahara, T. Nagao, I. Matsuda, G. Bihlmayer, E. V. Chulkov, Y. M. Koroteev, P. M. Echenique, M. Saito, and S. Hasegawa, Role of spin-orbit coupling and hybridization effects in the electronic structure of ultrathin Bi films, *Phys. Rev. Lett.* **97**, 146803 (2006).

[12] A. Varykhalov, D. Marchenko, M. R. Scholz, E. D. L. Rienks, T. K. Kim, G. Bihlmayer, J. Sánchez-Barriga, and O. Rader, Ir(111) surface state with giant Rashba splitting persists under graphene in air, *Phys. Rev. Lett.* **108**, 066804 (2012).

[13] J. H. Dil, F. Meier, J. Lobo-Checa, L. Patthey, G. Bihlmayer, and J. Osterwalder, Rashba-type spin-orbit splitting of quantum well states in ultrathin Pb films, *Phys. Rev. Lett.* **101**, 266802 (2008).

[14] P. D. C. King, R. C. Hatch, M. Bianchi, R. Ovsyannikov, C. Lupulescu, G. Landolt, B. Slomski, J. H. Dil, D. Guan, J. L. Mi, E. D. L. Rienks, J. Fink, A. Lindblad, S. Svensson, S. Bao, G. Balakrishnan, B. B. Iversen, J. Osterwalder, W. Eberhardt, F. Baumberger, and P. Hofmann, Large tunable Rashba spin splitting of a two-dimensional electron gas in Bi<sub>2</sub>Se<sub>3</sub>, *Phys. Rev. Lett.* **107**, 096802 (2011).

[15] Z.-H. Zhu, G. Levy, B. Ludbrook, C. N. Veenstra, J. A. Rosen, R. Comin, D. Wong, P. Dosanjh, A. Ubaldini, P. Syers, N. P. Butch, J. Paglione, I. S. Elfimov, and A. Damascelli, Rashba spin-splitting control at the surface of the topological insulator Bi<sub>2</sub>Se<sub>3</sub>, *Phys. Rev. Lett.* **107**, 186405 (2011).

[16] C. R. Ast, J. Henk, A. Ernst, L. Moreschini, M. C. Falub, D. Pacilé, P. Bruno, K. Kern, and M. Grioni, Giant spin splitting through surface alloying, *Phys. Rev. Lett.* **98**, 186807 (2007).

[17] I. Gierz, T. Suzuki, E. Frantzeskakis, S. Pons, S. Ostain, A. Ernst, J. Henk, M. Grioni, K. Kern, and C. R. Ast, Silicon surface with giant spin splitting, *Phys. Rev. Lett.* **103**, 046803 (2009).

[18] J. R. Bindel, M. Pezzotta, J. Ulrich, M. Liebmann, E. Y. Sherman, and M. Morgenstern, Probing variations of the Rashba spin-orbit coupling at the nanometre scale, *Nature Physics* **12**, 920 (2016).

[19] K. Ishizaka, M. S. Bahramy, H. Murakawa, M. Sakano, T. Shimojima, T. Sonobe, K. Koizumi, S. Shin, H. Miyahara, A. Kimura, K. Miyamoto, T. Okuda, H. Namatame, M. Taniguchi, R. Arita, N. Nagaosa, K. Kobayashi, Y. Murakami, R. Kumai, Y. Kaneko, Y. Onose, and Y. Tokura, Giant Rashba-type spin splitting in bulk BiTeI, *Nature Materials* **10**, 521 (2011).

[20] D. Di Sante, P. Barone, R. Bertacco, and S. Picozzi, Electric control of the giant Rashba effect in bulk GeTe, *Advanced Materials* **25**, 509 (2013).

[21] M. Liebmann, C. Rinaldi, D. Di Sante, J. Kellner, C. Pauly, R. N. Wang, J. E. Boschker, A. Giussani, S. Bertoli, M. Cantoni, *et al.*, Giant Rashba-type spin splitting in ferroelectric GeTe (111), *Advanced Materials* **28**, 560 (2016).

[22] Y. Ma, Y. Dai, W. Wei, X. Li, and B. Huang, Emergence of electric polarity in BiTeX (X= Br and I) monolayers and the giant Rashba spin splitting, *Physical Chemistry Chemical Physics* **16**, 17603 (2014).

[23] K. S. Novoselov, A. K. Geim, S. V. Morozov, D. Jiang, Y. Zhang, S. V. Dubonos, I. V. Grigorieva, and A. A. Firsov, Electric field effect in atomically thin carbon films, *Science* **306**, 666 (2004).

[24] P. Ajayan, P. Kim, and K. Banerjee, Two-dimensional van der Waals materials, *Physics Today* **69**, 38 (2016).

[25] K. S. Novoselov, A. Mishchenko, A. Carvalho, and A. H. Castro Neto, 2D materials and van der Waals heterostructures, *Science* **353**, aac9439 (2016).

[26] H. Fang, C. Battaglia, C. Carraro, S. Nemsak, B. Ozdol, J. S. Kang, H. A. Bechtel, S. B. Desai, F. Kronast, A. A. Unal, *et al.*, Strong interlayer coupling in van der Waals heterostructures built from single-layer chalcogenides, *Proceedings of the National Academy of Sciences*

111, 6198 (2014).

[27] H. Kasai, K. Tolborg, M. Sist, J. Zhang, V. R. Hathwar, M. Ø. Filsø, S. Cenedese, K. Sugimoto, J. Overgaard, E. Nishibori, *et al.*, X-ray electron density investigation of chemical bonding in van der Waals materials, *Nature materials* **17**, 249 (2018).

[28] Q. Liu, Y. Guo, and A. J. Freeman, Tunable Rashba effect in two-dimensional LaOBiS<sub>2</sub> films: Ultrathin candidates for spin field effect transistors, *Nano letters* **13**, 5264 (2013).

[29] S. Singh and A. H. Romero, Giant tunable rashba spin splitting in a two-dimensional BiSb monolayer and in BiSb/AlN heterostructures, *Phys. Rev. B* **95**, 165444 (2017).

[30] Q. Zhang and U. Schwingenschlögl, Rashba effect and enriched spin-valley coupling in GaX/MX<sub>2</sub> (M=Mo,W; X=S,Se,Te) heterostructures, *Phys. Rev. B* **97**, 155415 (2018).

[31] Y. Wang, L. Li, W. Yao, S. Song, J. T. Sun, J. Pan, X. Ren, C. Li, E. Okunishi, Y.-Q. Wang, E. Wang, Y. Shao, Y. Y. Zhang, H.-t. Yang, E. F. Schwier, H. Iwasawa, K. Shimada, M. Taniguchi, Z. Cheng, S. Zhou, S. Du, S. J. Pennycook, S. T. Pantelides, and H.-J. Gao, Monolayer PtSe<sub>2</sub>, a new semiconducting transition-metal-dichalcogenide, epitaxially grown by direct selenization of Pt, *Nano Letters* **15**, 4013 (2015).

[32] Y. Zhao, J. Qiao, Z. Yu, P. Yu, K. Xu, S. P. Lau, W. Zhou, Z. Liu, X. Wang, W. Ji, *et al.*, High-electron-mobility and air-stable 2D layered PtSe<sub>2</sub> fets, *Advanced Materials* **29**, 1604230 (2017).

[33] W. Yao, E. Wang, H. Huang, K. Deng, M. Yan, K. Zhang, K. Miyamoto, T. Okuda, L. Li, Y. Wang, *et al.*, Direct observation of spin-layer locking by local Rashba effect in monolayer semiconducting PtSe<sub>2</sub> film, *Nature communications* **8**, 14216 (2017).

[34] X. Zhang, Q. Liu, J.-W. Luo, A. J. Freeman, and A. Zunger, Hidden spin polarization in inversion-symmetric bulk crystals, *Nature Physics* **10**, 387 (2014).

[35] L. Yuan, Q. Liu, X. Zhang, J.-W. Luo, S.-S. Li, and A. Zunger, Uncovering and tailoring hidden Rashba spin-orbit splitting in centrosymmetric crystals, *Nature communications* **10**, 906 (2019).

[36] M. A. U. Absor, I. Santoso, Harsojo, K. Abraha, H. Kotaka, F. Ishii, and M. Saito, Strong Rashba effect in the localized impurity states of halogen-doped monolayer PtSe<sub>2</sub>, *Phys. Rev. B* **97**, 205138 (2018).

[37] Y.-H. Chang, W. Zhang, Y. Zhu, Y. Han, J. Pu, J.-K. Chang, W.-T. Hsu, J.-K. Huang, C.-L. Hsu, M.-H. Chiu, *et al.*, Monolayer MoSe<sub>2</sub> grown by chemical vapor deposition for fast photodetection, *ACS nano* **8**, 8582 (2014).

[38] J. Reyes-Retana and F. Cervantes-Sodi, Spin-orbital effects in metal-dichalcogenide semiconducting monolayers, *Scientific reports* **6**, 24093 (2016).

[39] D. Xiao, G.-B. Liu, W. Feng, X. Xu, and W. Yao, Coupled spin and valley physics in monolayers of MoS<sub>2</sub> and other group-VI dichalcogenides, *Phys. Rev. Lett.* **108**, 196802 (2012).

[40] Y. K. Luo, J. Xu, T. Zhu, G. Wu, E. J. McCormick, W. Zhan, M. R. Neupane, and R. K. Kawakami, Opto-valleytronic spin injection in monolayer MoS<sub>2</sub>/few-layer graphene hybrid spin valves, *Nano letters* **17**, 3877 (2017).

[41] G. Kresse and D. Joubert, From ultrasoft pseudopotentials to the projector augmented-wave method, *Phys. Rev. B* **59**, 1758 (1999).

[42] J. P. Perdew, K. Burke, and M. Ernzerhof, Generalized gradient approximation made simple, *Phys. Rev. Lett.* **77**, 3865 (1996).

[43] S. Grimme, J. Antony, S. Ehrlich, and H. Krieg, A consistent and accurate *ab initio* parametrization of density functional dispersion correction (DFT-D) for the 94 elements H-Pu, *The Journal of Chemical Physics* **132**, 154104 (2010).

[44] Z. Y. Zhu, Y. C. Cheng, and U. Schwingenschlögl, Giant spin-orbit-induced spin splitting in two-dimensional transition-metal dichalcogenide semiconductors, *Phys. Rev. B* **84**, 153402 (2011).

[45] J. Kang, J. Li, S.-S. Li, J.-B. Xia, and L.-W. Wang, Electronic structural moiré pattern effects on MoS<sub>2</sub>/MoSe<sub>2</sub> 2d heterostructures, *Nano Lett.* **13** (2013).

[46] H.-P. Komsa and A. V. Krasheninnikov, Electronic structures and optical properties of realistic transition metal dichalcogenide heterostructures from first principles, *Phys. Rev. B* **88**, 085318 (2013).

[47] X. Su, W. Ju, R. Zhang, C. Guo, J. Zheng, Y. Yong, and X. Li, Bandgap engineering of MoS<sub>2</sub>/MX<sub>2</sub> (MX<sub>2</sub>=WS<sub>2</sub>, MoSe<sub>2</sub> and WSe<sub>2</sub>) heterobilayers subjected to biaxial strain and normal compressive strain, *RSC Advances* **6**, 18319 (2016).

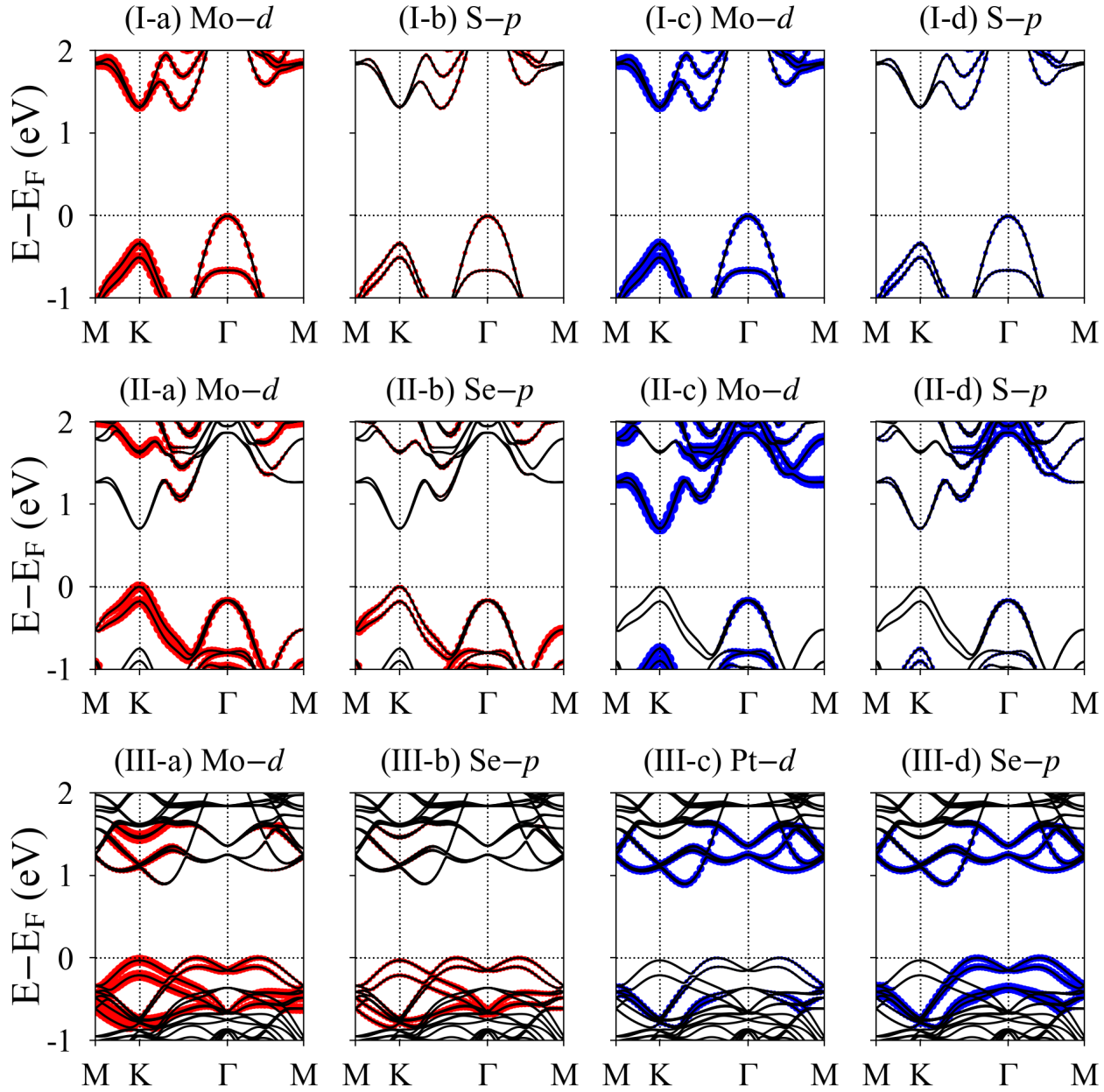
[48] C. Gong, H. Zhang, W. Wang, L. Colombo, R. M. Wallace, and K. Cho, Band alignment of two-dimensional transition metal dichalcogenides: Application in tunnel field effect transistors, *Applied Physics Letters* **103**, 053513 (2013).

# Supplementary Materials for "Tunable Giant Rashba-type Spin Splitting in PtSe<sub>2</sub>/MoSe<sub>2</sub> Heterostructure"

Longjun Xiang, Youqi Ke, and Qingyun Zhang\*

*School of Physical Science and Technology, ShanghaiTech University, Shanghai, 201210, China*

(Dated: May 4, 2022)



\* zhangqy2@shanghaitech.edu.cn

FIG. 1. Band structures with projections to different atomic orbitals for (I) bilayer MoS<sub>2</sub>, (II) MoSe<sub>2</sub>/MoS<sub>2</sub> and (III) PtSe<sub>2</sub>/MoSe<sub>2</sub> heterostructures. Here the size of circles represents the contribution of atomic orbitals. The red and blue colors represent two constituent layers. In the following, we adopt the same convention.

In FIG.1, we compare the features of orbital hybridization around  $\Gamma$  point for the atomic-orbitals in bilayer MoS<sub>2</sub>, MoSe<sub>2</sub>/MoS<sub>2</sub> and PtSe<sub>2</sub>/MoSe<sub>2</sub>. It is found that the hybridization in bilayer MoS<sub>2</sub> and MoSe<sub>2</sub>/MoS<sub>2</sub> is dominated by the Mo-*d* orbitals from different layers, as shown in FIG.1 (I-a), (I-c), (II-a) and (II-c). However, the hybridization around  $\Gamma$  point in PtSe<sub>2</sub>/MoSe<sub>2</sub> is mainly contributed by Mo-*d* orbitals in MoSe<sub>2</sub> layer and Se-*p* orbitals in PtSe<sub>2</sub>, which shows a distinct feature compared to bilayer MoS<sub>2</sub> and MoS<sub>2</sub>/MoSe<sub>2</sub>. This emerging hybridization results in the giant Rashba-type spin splitting in PtSe<sub>2</sub>/MoSe<sub>2</sub>, as discussed in the main manuscript.

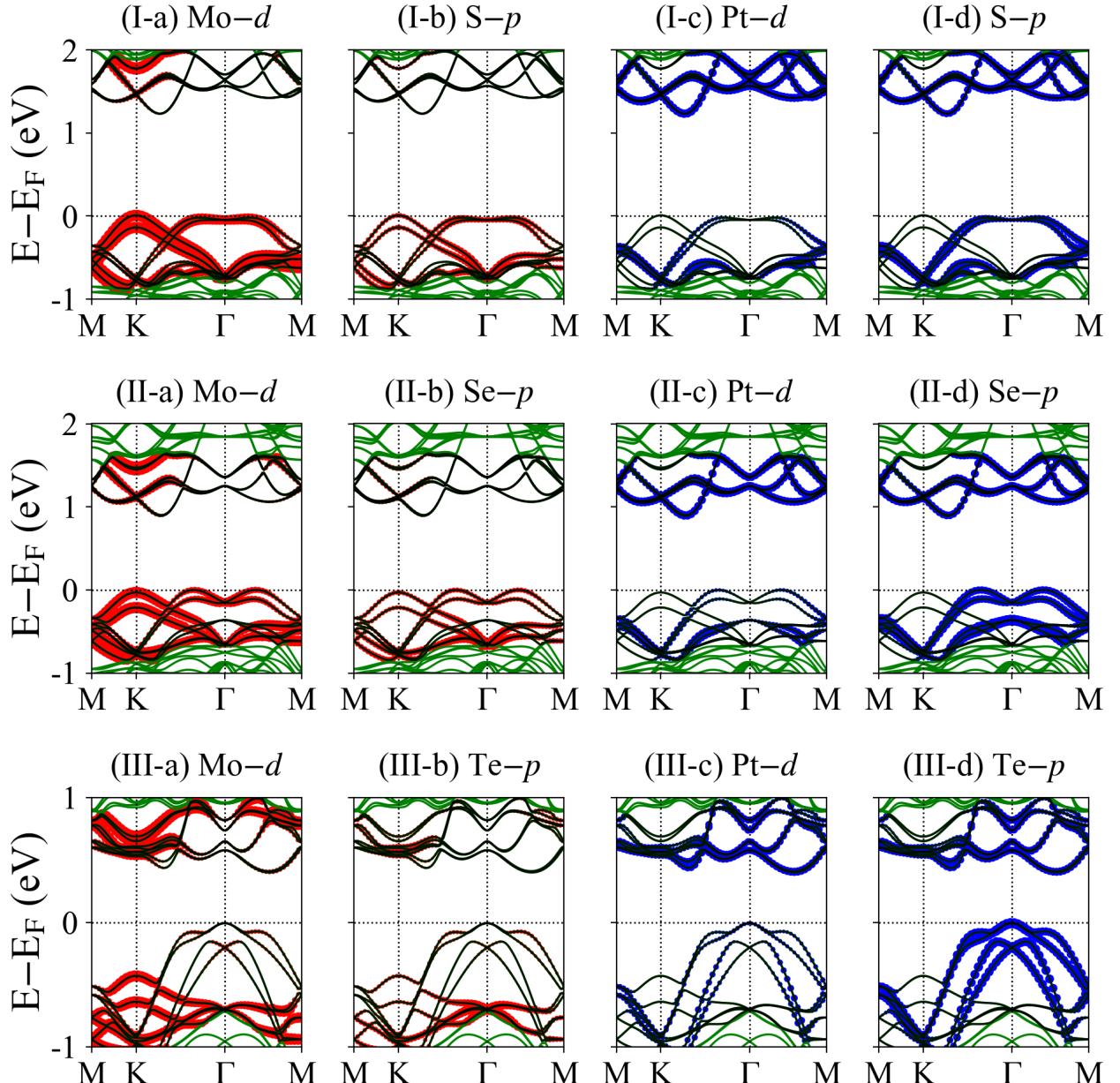


FIG. 2. The band structures of (I) PtS<sub>2</sub>/MoS<sub>2</sub>, (II) PtSe<sub>2</sub>/MoSe<sub>2</sub>, and (III) PtTe<sub>2</sub>/MoTe<sub>2</sub> with projections to the corresponding atomic orbitals for the bands near Fermi level.

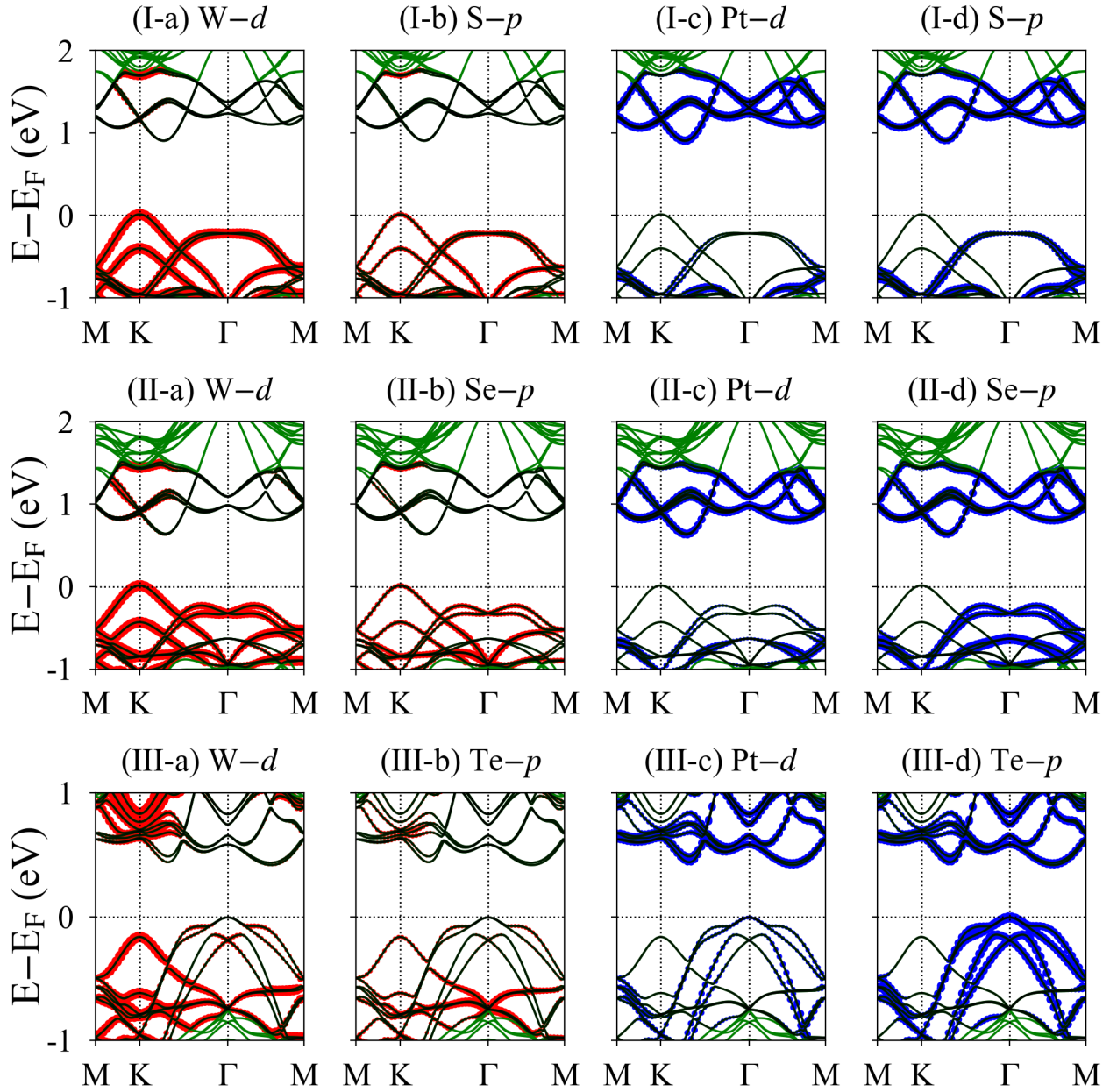


FIG. 3. The band structures of (I)  $\text{PtS}_2/\text{WS}_2$ , (II)  $\text{PtSe}_2/\text{WSe}_2$ , and (III)  $\text{PtTe}_2/\text{WTe}_2$  with projections to the corresponding atomic orbitals for the bands near Fermi level.

In FIG.2 and FIG.3, we present the band structures and features of orbital hybridization for the  $\text{PtX}_2/\text{MoX}_2$  and  $\text{PtX}_2/\text{WX}_2$  ( $\text{X}=\text{S, Se, Te}$ ), respectively. As shown in FIG.2 (I) and (II), we observe similar hybridization features for  $\text{PtS}_2/\text{MoS}_2$  and  $\text{PtSe}_2/\text{MoSe}_2$ , but the band splitting around  $\Gamma$  point in  $\text{PtS}_2/\text{MoS}_2$  is much smaller due to the weaker spin-orbit coupling in S atom. While for  $\text{PtTe}_2/\text{MoTe}_2$  shown in FIG.2 (III), almost no  $p$ - $d$  hybridization and no band splitting around  $\Gamma$  point is observed at VBE. Substituting Mo atoms with W atoms in these heterostructures will bring about two main changes to their band structures, as shown in FIG.3. Firstly, the band splitting of VBE at  $K$  point become larger due to the stronger SOC in W atom than that in Mo atom. Secondly, the energy levels of VBE around  $\Gamma$  point are suppressed compared to those at  $K$  point. However, the orbital hybridizations in  $\text{PtX}_2/\text{WX}_2$  are almost the same as in  $\text{PtX}_2/\text{MoX}_2$ .